



B6 - Minerals

B6 - O1

THE BLUE MINERAL PIGMENT AERINITE STUDIED AT HIGH TEMPERATURE WITH LABORATORY POWDER DIFFRACTION DATA

Jordi Rius¹, Xavier Alcobé²

¹*Inst. Ciència de Materials de Barcelona (CSIC), Campus UAB, 08193 Bellaterra, Catalunya, Spain*

²*Serveis Científicotècnics, Univ. de Barc., Lluís Solé i Sabarís 1, 08028 Barcelona, Catalunya, Spain.*

The structure of aerinite, a blue fibrous silicate mineral associated with the alteration of ophitic rocks in the southern Pyrenees has been recently determined by applying the direct methods modulus sum function to synchrotron powder diffraction data [1]. This mineral is the blue pigment commonly used in most Catalan romanica paintings between the XIV-XV centuries. The unit cell dimensions of aerinite are $a = b = 16.8820(9) \text{ \AA}$, $c = 5.2251(3) \text{ \AA}$, the space group is $P3c1$ and the approximate structural formula is $\text{Ca}_5(\text{Fe}^{3+}, \text{Fe}^{2+}_2, \text{Al})(\text{Al}_5 \text{Mg})[\text{Si}_{12}\text{O}_{36}(\text{OH})_{12}\text{H}]$ with $Z=1$. The crystal structure of aerinite can be best understood by introducing cylindrical basic building units consisting on three pyroxene chains pointing inwards to accommodate tri- and divalent cations at the centre of the resulting face-sharing octahedra. The mean cation-oxygen bond length is 2.04 \AA and the intercationic distance is 2.61 \AA . Out of the three symmetry-independent three-fold rotation axes in the unit cell, two are occupied by such cylindrical units and the third by CO_3 groups. Consequently, each unit is surrounded by three similar ones which are, however, shifted by 0.93 \AA along c . Between such units, i.e. tangential to both cylindrical envelopes, a four-row wide slab of a brucite layer is found. The two inner octahedra are predominantly filled with Al and Mg atoms, the two outer with Ca and Na. The internal O atoms of the brucite-like layers are hydroxyl groups, the intermediate are unshared basal O atoms of the neighbouring pyroxene chains, while the external ones are water molecules forming relatively strong H-bridges with the partially disordered CO_3 groups (Figure 1).

One peculiar property of aerinite that has been confirmed by infrared spectroscopy and TG measurements, is the loss of the CO_3 groups when heated at $300 \text{ }^\circ\text{C}$. When cooled down, however, aerinite slowly absorbs CO_2 from the atmosphere and, at the end, the resulting structure is identical to the initial one. This zeolitic behaviour neces-

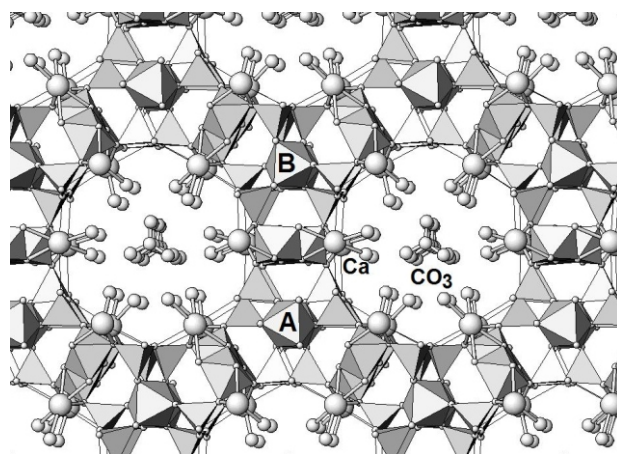


Figure 1

sarily involves a rearrangement of the coordination polyhedra. To study this reversible transformation, the same sample previously measured at the synchrotron was measured again at $25 \text{ }^\circ\text{C}$ and $300 \text{ }^\circ\text{C}$ on a laboratory X-ray powder diffractometer. On the basis of these two patterns, the mechanism that helps to stabilise the high temperature form of aerinite could be successfully derived from the corresponding Rietveld refinements. It has been found that both low and high temperature forms have the same non centrosymmetrical space group $P3c1$. The crystal structure of the high temperature form will be described in detail.

Acknowledgement

This study was supported by the Ministerio de Ciencia y Tecnología, Project Number: MAT2002-02808.

- [1] J.Rius, E.Elkaim, X. Torrelles, *Eur.J.Mineral.* 16 (2004) 127-134.

B6 - O2

SYNCHROTRON RADIATION XRPD STUDY OF NON IDEALITY, THERMAL EXPANSION AND INCOMMENSURATE-NORMAL STRUCTURE PHASE TRANSITION IN MELILITES

Marco Merlini¹, Mauro Gemmi¹, Gilberto Artioli¹

¹*Dipartimento di Scienze della Terra "A. Desio", Università degli Studi di Milano, Italy*

Melilites are a group of minerals which form continuous solid solutions between the end members gehlenite (Ge, $\text{Ca}_2\text{Al}_2\text{SiO}_7$) akermanite (Ak, $\text{Ca}_2\text{MgSi}_2\text{O}_7$), soda-melilite (NaMel, $\text{NaCaAlSi}_2\text{O}_7$) and Fe-bearing end members (Fe^{2+} -gehlenite – Fe^{3+} -gehlenite / Fe^{2+} -akermanite – Fe^{3+} -akermanite). The importance of these minerals is due to the fact that almost pure terms of the series gehlenite-akermanite are among the first silicates which condensed from the solar nebula and they are found in chondritic meteorites. Melilites crystallise also in alkaline magmatic rocks, whose origin is restricted to significant geodynamic environments. Therefore a modelling of their thermodynamic parameters is mandatory in order to improve the accuracy of phase equilibria calculations, which could have important implications in petrological studies (i.e. for accurate determination of the thermal history of meteorites, of the temperature of solidification of alkaline rocks ...). The thermodynamic calculations involving phase equilibria of melilites are usually performed assuming the ideality of the solid solution (s.s.) [1]. Nevertheless melilite s.s. has not an ideal behaviour (fig. 1). Our results show that the unit cell volume curve in the ge-ak join has a sigmoidal shape, with a negative and a positive excess molar volume close to ge and ak end-members respectively. This is the general behaviour of non equivalent site substitution mentioned by Newton and Wood [2] for binary silicate solid solutions. An other important feature of melilites is the presence of an incommensurate modulated (IC) structure, especially for ak-rich compositions, which transforms into a normal (N) one upon heating [3, 4, 5]. The temperature of IC-N phase transition is of 80 °C for pure akermanite and it is increased by Fe/Mg substitution and decreased by Al/(Mg+Si) exchange. We performed high

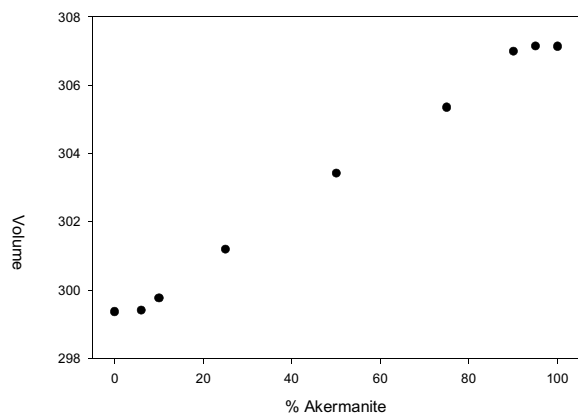


Fig. 1 - Volume (Å^3) in the join Ge-Ak at 300 K with the characteristic S-shaped form of the volume curve in binary silicate solid solutions.

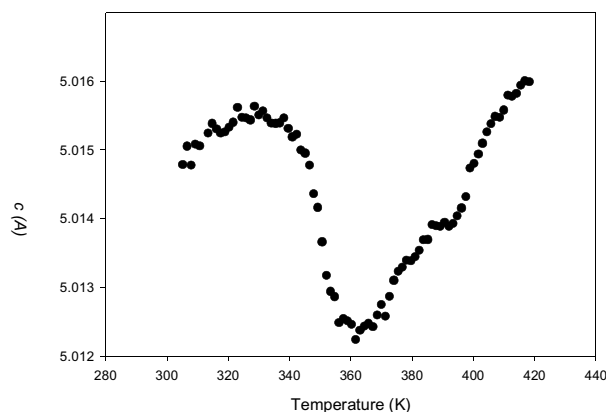


Fig. 2 - Variation of c lattice parameter value across the phase transition for akermanite measured with T.I.P. detector at GILDA beamline (ESRF).

temperature (HT) X-ray powder diffraction (XRPD) on terms of Ge-Ak-NaMel on the italian CRG beamline BM08 (GILDA) at ESRF, Grenoble in order to measure reliable thermodynamics data (volume, thermal expansion) for several composition and to investigate the IC-N phase transition for some terms near Ak end-member. The experiments were performed with monochromatic radiation; the samples were contained in quartz glass capillary, heated with a hot gas blower and data were collected with a translating image plate (T.I.P.) [6]. IC and N phases are marked by a strong difference in thermal expansion along the main crystallographic directions. Thermal expansion measure-

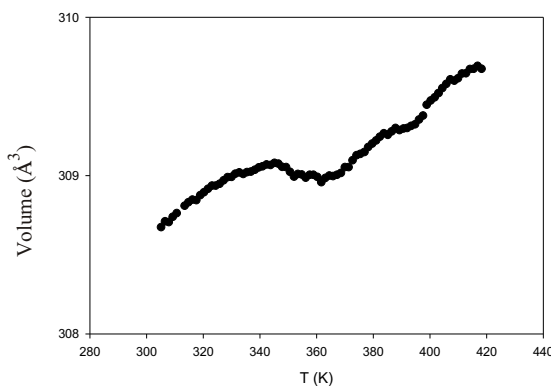


Fig. 3 - Thermal expansion of akermanite across the IC-N phase transition



ments allowed to investigate the field stability of IC phase near ak composition. The phase transition is characterised by a contraction along c and also a slight negative volumetric expansion (fig. 2-3). The results obtained comprise also accurate thermal expansion measurements and crystal-structure Rietveld refinements for melilites in Ak-Ge and Ak-NaMel joins in the temperature range 270-1300 K.

[1] Yoneda S. & Grossman L., 1995, *Geoch. Cosmoch. Acta*, 59, (16), 3413-3444.

[2] Newton R.C. & Wood B., 1980, *Am. Mineral.*, 65, 733-745.

[3] Seifert et al., 1987, *Phys. Chem. Minerals*, 14, 26-35.

[4] Rothlisberger et al., 1990, *Eur. J. Mineral.*, 2, 585-594.

[5] Yang et al., 1997, *Phys. Chem. Minerals*, 24, 510-519.

[6] Meneghini et al., 2001, *Journ. Synchrotron. Rad.* 8, 1162-1166.

B6 - O3

IN SITU ANOMALOUS POWDER DIFFRACTION STUDY OF CATION DISTRIBUTIONS IN BICATIONIC ZEOLITES

H. Palancher^{1,2}, J.L. Hodeau², C. Pichon¹, J.F. Bézar^{2,3}, J. Lynch¹, B. Rebours¹ and J. Rodriguez-Carvajal⁴

¹Lab. de cristallographie, CNRS BP166X 38042 Grenoble, France

²Institut Français du Pétrole, BP3 69390 Vernaison, France

³French CRG D2AM, ESRF, BP220 38043 Grenoble, France

⁴Lab. Léon Brillouin, CEA/Saclay, 91191 Gif/Yvette, France

Adsorption properties of molecular sieves such as X, Y or A zeolites are widely used in industrial processes (in particular for separation and purification of hydrocarbon isomers). Adsorption selectivity of these materials depends highly on the type, the number and the location of cations in the structure where they compensate the negative charge of the framework. The study of the cation distributions on each site, under adsorption conditions close to their industrial use, is of great interest in the search of better molecular sieves which could be bicationic zeolites. In this work two methodological aspects will be presented: first the *in situ* instrumentation and second the advances in anomalous powder diffraction data analysis (required for cation distributions determination in bicationic zeolites) illustrated by the study of CaSrX and SrRbX zeolitic samples.

A cell has been especially designed for the X-ray diffraction (XRD) study of powders under gas or liquid flow,

at various temperatures and pressures [1, 2]. It mainly consists of:

- a reactor whose geometry enables fix bed flow,
- a miniaturised cylindrical furnace ensuring an extremely low thermal gradient (smaller than 1°C over a 6 mm zone along the capillary at 250°C).

The limited size of this cell has enabled its installation on a synchrotron radiation beamline (D2AM at the ESRF). Thanks to this set-up, reproducible and high quality diffraction data can be measured (cf. figure 1).

In the faujasite structure, cations occupy known sites. In bicationic zeolites, two different cations are located in very close crystallographic positions. If presence of both Sr⁺⁺ and Rb⁺ cations on site II in dehydrated SrRbX can be suggested from electron density map (figure II-B), this technique appears inefficient when trying to determine Sr⁺⁺ and Ca⁺⁺ cation locations in dehydrated SrCaX: since elec-

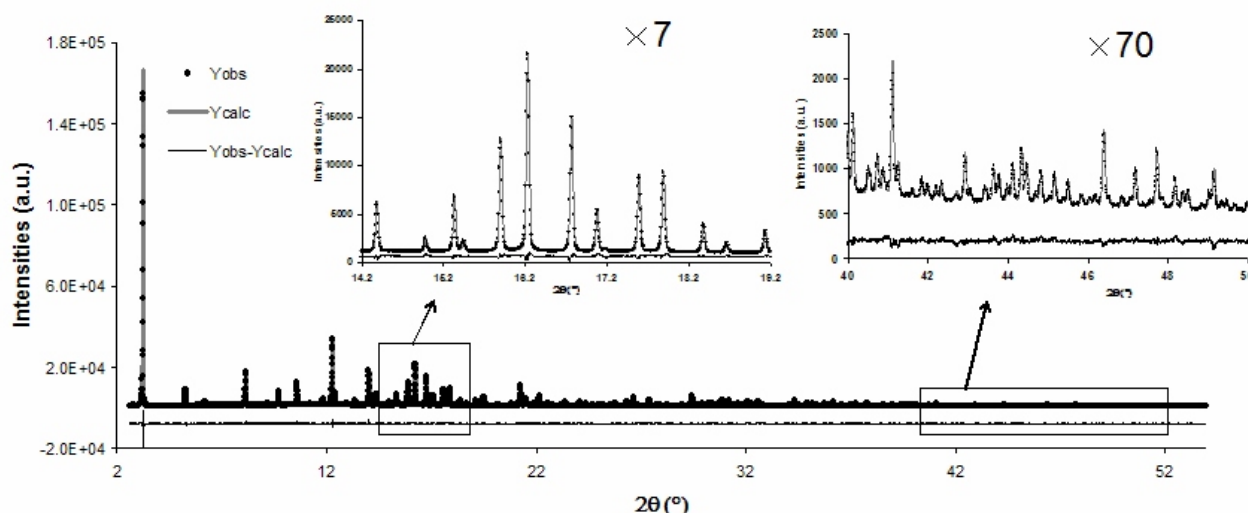


Figure 1: Calculated and measured powder diffraction pattern on water saturated CaSrX (E=15.192keV).

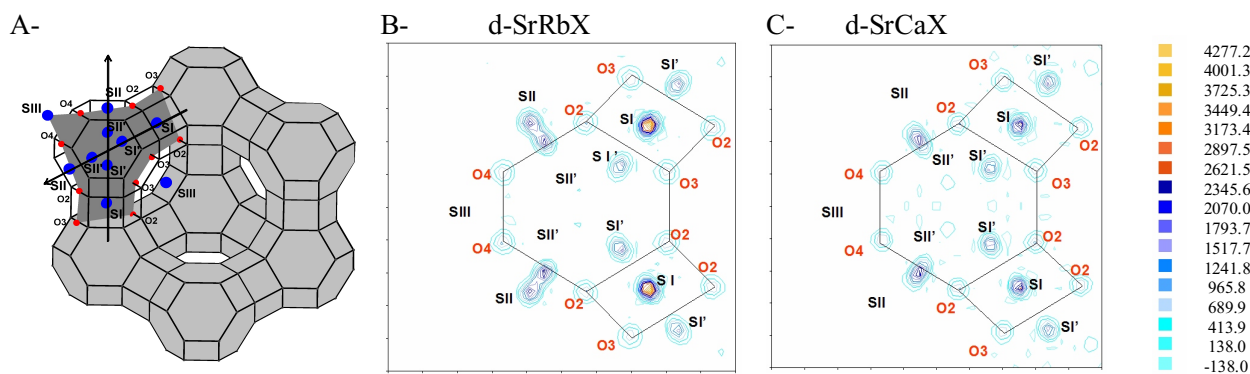


Figure 2: Study of degeneracy of cation site (for example site II) on electronic density maps calculated with Fourier transforms in the P plane (represented in dark grey in the faujasite structure) (A-) in two dehydrated samples SrRbX (B-) and CaSrX (C-).

tronic densities due to Ca^{++} coincide with those of Sr^{++} , no site degeneracy can be observed. This kind of problem can be encountered in certain monocationic hydrated zeolites since water molecules can be adsorbed near cationic sites.

Anomalous effect could be used to distinguish these species. This phenomenon leads to strong variations with energy of the atomic scattering factor of an element under an X-ray beam of energy close to one of its absorption edges. However multi-wavelength measurements require new synchrotron sources to be performed in good conditions. Diffraction patterns have been collected over a wide angular range ($\sin \theta / \lambda = 0.57 \text{ \AA}^{-1}$ at least) at 15192 eV (about 900 eV under strontium K absorption edge ($E_K(\text{Sr}) - 900\text{eV}$)) and at 16096 eV ($E_K(\text{Sr}) - 10\text{eV}$) on SrCaX. A methodology for anomalous powder diffraction data analysis has been established including simultaneous refinement of all diffraction patterns using Fullprof software package [3]. Its efficiency has been validated by the determination Sr^{++} and Rb^+ cation distributions in SrRbX sample [4, 5]. This study was a particularly difficult case for X-ray diffraction since Rb^+ and Sr^{++} have the same scattering power ($Z_{\text{Rb}^+} = Z_{\text{Sr}^{++}} = 35\text{e.u.}$). Note that, as Rb and Sr have similar neutron scattering lengths ($b_{\text{Rb}} \approx b_{\text{Sr}} \approx 0.7 \cdot 10^{-12} \text{ cm}^{-1}$), neutron diffraction will not help us in this case.

CaSrX sample has been characterised at two hydration levels: water saturated (measurement *ex situ* at 20°C) and highly dehydrated (measurement *in situ* under dry nitrogen flow at 250°C). Results of the refinements show the expected strong cation motions with water molecules loss [2] (figure III). If the very close distributions of Sr^{++} and Ca^{++} cations in the dehydrated sample could have been predicted from chemical considerations (close cationic radii and same electric charge), the very different behaviour of these cations in water saturated case underlines the complexity of bicationic zeolites. Importance of accurate measurements on these systems is demonstrated.

1. Palancher, H., Pichon, C., Prévot, S., Conan, G., Hodeau, J.L and Berar, J.F. (2003) *Patent 03/07 641*.
2. Palancher, H., Pichon, C., Hodeau, J.L., Lynch, J., Rebours, B., Berar, J.F. *et al.* (2004) *submitted to JAC*.
3. Rodriguez-Carvajal, J. (2002). Fullprof version 2.10 LLB, CEA/Saclay, France, <http://www-llb.cea.fr/fullweb/poudres.htm>.
4. Hodeau, J.L., Nassif, V., Palancher, H., Berar, J.F., Dooryhee, J.F., Carbonio, E. *et al.* (2003) *ECM Durban*.
5. Palancher, H., Hodeau, J.L., Pichon, C., J. Lynch, Berar, J.F., Rebours, B. and Rodriguez-Carvajal, J. (2004) *submitted*.

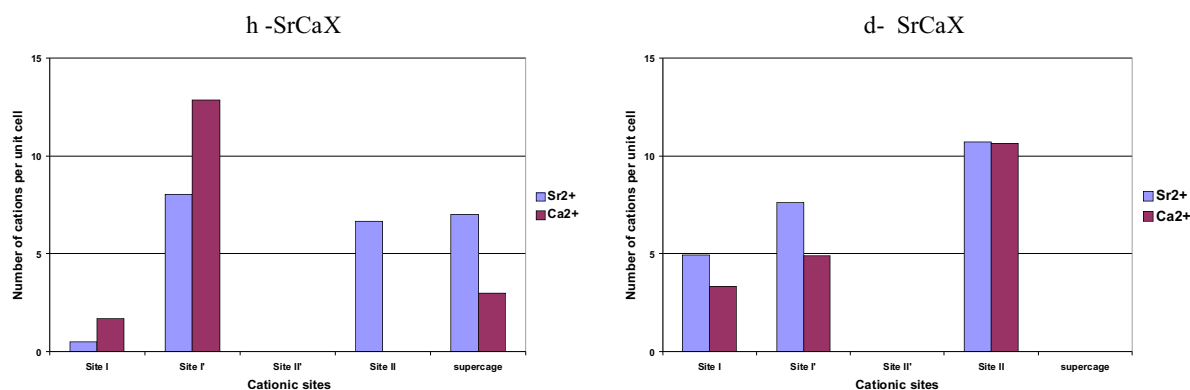


Figure 3: Sr^{++} and Ca^{++} cation distributions in SrCaX sample at two hydration levels: water saturated (h-SrCaX) and highly dehydrated (d-SrCaX).





B6 - O4

CRYSTAL STRUCTURE DETERMINATION OF ROSASITE AND MCGUINNESSITE

N. Perchiazzi

Department of Earth Sciences, Università di Pisa, Via S.Maria 53, 56126 Pisa, Italy

The carbonate group of malachite, with general formula $\text{Me}^{2+}_2(\text{CO}_3)(\text{OH})_2$, includes malachite ($\text{Me}^{2+} = \text{Cu}$), georgeite (Cu), glaukosphaerite (Cu,Zn), kolwezite (Cu,Co), mcguinnessite (Cu,Mg), nullagine (Ni), pokrovskite (Mg), rosasite (Cu,Zn). Besides the chemical composition, the structural relationships between these minerals are demonstrated by the similarity of their powder patterns. A constant feature of these minerals is their microcrystalline fibrous habit. This feature precluded in most cases single crystal studies, which could be performed for malachite and rosasite only. For the remaining phases, space group symmetry and cell parameters were mainly derived from powder pattern indexing. Apart from that of malachite (Zigan et al., 1977), no other structural determinations are available for the minerals of the malachite group.

Spheroidal aggregates of rosasite in extremely thin fibrous crystals from Ojuela mine, Durango, Mexico, were carefully hand picked under the binocular microscope and gently hand milled in an agate mortar under acetone, to fill with the resulting powder a 0.5 mm Lindemann capillary.

Powder diffraction data were collected on a Bruker D8 Vario diffractometer, equipped with a primary Ge (111) monochromator and a Braun PSD detector, working in capillary geometry. This configuration allowed us to use a carefully selected amount of material, as well as to reduce the strong preferred orientation due to the fibrous habit of rosasite. Two scans were acquired in the interval 11-60 and 60-100 2° , with step 0.016 $^\circ$ and counting times 24 and 48 s respectively.

The crystal structure of rosasite was solved through the EXPO (Altomare et al., 1999) program. A trial with a malachite-like starting model gave no results, whereas assuming the space group and the cell constants gave in the single crystal study by Roberts et al. (1986), we obtained a promising starting structural model. This model was completed through the subsequent Rietveld refinement, performed through the GSAS/EXPGUI suite of programs (Larson and von Dreele, 2000; Toby, 2001). The refined cell parameters were $a = 12.8976(3)$, $b = 9.3705(1)$, $c = 3.1622(1)$ Å, $\beta = 110.260(3)^\circ$, space group $P2_1/a$.

In the early stages of the refinement, constraints on the Me-O bonds were introduced and finally removed. The carbonate group was refined as a rigid body, imposing a C-O distance of 1.3 Å and a common isotropic displacement parameter for the atoms of the group. Isotropic displacement parameters were assumed also for the remaining atoms. The Rietveld refinement finally converged to $R_{wp} = 10.38\%$, $R_p = 0.0751$ (powder totals) and $RF^2 = 6.12, 6.33\%$ (for the two used datasets).

The experimental data for mcguinnessite were acquired in the same conditions as for rosasite, and its crystal structure was successfully solved using the rosasite structure as

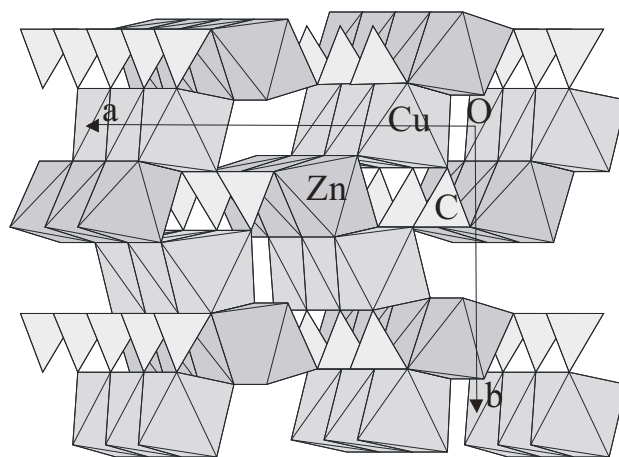


Figure 1: The crystal structure of rosasite, as parallel to (001). In Mcguinnessite we find Mg instead of Zn, and the Cu site is partially filled by Mg.

a starting model. Trials to solve mcguinnessite through a malachite-structure model failed. The refined cell parameters for mcguinnessite were $a = 12.8978(6)$, $b = 9.3737(4)$, $c = 3.1558(2)$ Å, $\beta = 111.225(4)^\circ$, space group $P2_1/a$.

The Rietveld refinement (GSAS/EXPGUI package) finally converged to $R_{wp} = 8.06\%$, $R_p = 0.0578$ (powder totals) and $RF^2 = 5.46, 5.16\%$ (for the two used datasets). The two minerals are isostructural, and the two independent metal sites are occupied in rosasite by Cu (the more distorted polyhedron) and by $\text{Zn}_{0.8}\text{Cu}_{0.2}$, in mcguinnessite by $\text{Cu}_{0.82}\text{Mg}_{0.18}$ and $\text{Mg}_{0.9}\text{Cu}_{0.1}$. The crystal structure of rosasite is reported in Fig. 1, as seen parallel to (001) plane.

Both the Zn and the Cu octahedra share edges forming Cu-based and Zn-based octahedral “columns”, running along [001], and responsible for the acicular habit of the mineral.

These octahedral “columns” form by edge-sharing octahedral “ribbons”, two columns large, are directly connected by apex-sharing and through the carbonate groups, each carbonate being linked to three octahedral ribbons.

Altomare, A., Burla, M.C., Cavalli, M., Carrozzini, B., Cascarano, G.L., Giacovazzo, C., Gagliardi, A., Moliterni, G. G., Polidori, G., & Rizzi, R. (1999): *J. Appl. Cryst.* (1999). **32**, 339-340

Larson, A.C. and Von Dreele, R.B. (2000): General structure analysis system (GSAS) Los Alamos National Laboratory Report LAUR 86-748. Roberts, A. C., Jambor, J. L., Grice, J. D. (1986): The X-ray crystallography of rosasite from Tsumeb, Namibia. *Powder Diffraction*, **1**, 56-57.

Toby, B.H. (2001): *J. Appl. Cryst* **34**, 210-221.

Zigan, F., Joswig, W., Schuster, H.D., Mason, S.A. (1977) *Zeitschrift für Kristallographie* **145** (1977), 412-426.

THE EGG-SHELL MICROSTRUCTURE STUDIED BY POWDER DIFFRACTION

L. Dobiášová^{†1}, R. Kužel¹, H. Šichová¹, J. Kopeček²¹Faculty of Mathematics and Physics, Charles University, Ke Karlovu 5, 121 16 Praha 2, Czech Republic²Institute of Physics, Academy of Sciences of the Czech Republic[†] in memoriam

In last years, traditional technique of powder diffraction known mainly to materials scientists, physicists, chemists, mineralogists is also applied to biological materials. First powder diffraction studies of protein structures has appeared [1, 2]. However, powder diffraction is known also as a suitable tools for studies of the so-called real structure of materials. In present work, we have tried to perform more complete diffraction analysis of different egg-shells.

The biological function of the egg-shell is a chamber for embryonic development and from which the chick is able to emerge at the appropriate time. The requirements of the table egg industry are different. The industry sustains economic loss from cracked eggs and some of the cracking can be attributed to the deficiencies in the egg-shell structure. This is one of the reasons why the attention to egg-shell is devoted [3-5].

The egg-shell consists of several mutually through-growing layers of CaCO₃. The inner most layer – mamillary layer (~100 μm) grows on the outer egg membrane and creates the base on which the palisade layer constitutes the thickest part (~200 μm) of the egg-shell. The top layer is the vertical layer (~5-8 μm) covered by the organic cuticle. Different kinds of hen's and bird's egg-shells in the powder form or as a whole from both sides of the shell were examined by powder diffractometry and film back-reflection method. The powder patterns were evaluated by the fitting of diffraction profiles with the Pearson VII function.

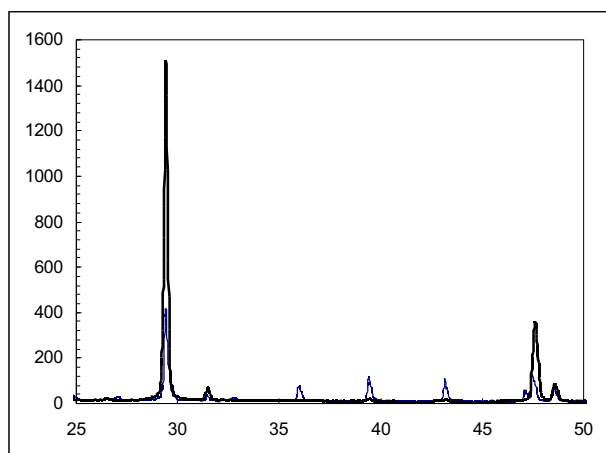


Figure 1. A typical part of the diffraction pattern of the egg-shell (CaCO₃) - from the inner (thin line) and outer side (thick line), respectively.

The lattice parameters, peak intensities and profile broadening were analysed. At the Bragg-Brentano setting ($2\theta = 40^\circ$) the Cu radiation penetrates approximately into the 9 μm of the egg-shell, so the measurements from the inner and outer shell surface can give evidence of the mamillary and palisade layer, respectively. The results obtained on egg-shells of very different origins shown no significant differences in lattice parameters that correspond well to the PDF-2 values. The patterns contained only basic phase CaCO₃ (space group no. 167: R-3c) with a small addition of magnesium (0.3 wt. %, determined by atomic absorption). Diffraction patterns of powders obtained from all the eggs investigated correspond very well to the pattern of standard CaCO₃. The correspondence is very good including intensities. The patterns obtained from egg-shell powders are also very similar to the standard pattern, regardless larger line broadening.

However, there are differences between powders and both sides of the shells. For inner shell surfaces, the intensities are only slightly different than in powders (including standard one) but there is significant line broadening indicating fluctuations of lattice spacings (the mean local strain of about 0.2 %). On the other hand, for outer shell surfaces, there is much smaller broadening of lines, similar to powders, but significant changes of intensities indicating the (001) textures of grains. This is also an evidence of presence of two basic layers, structurally very different – mamillary and palisade. The meaning of crystallographic texture has been emphasized [3, 4]. It was stated that the breaking strength of the egg shell is inversely related to the degree of calcite orientation and conversely, reduced strength in the egg shell from aged hens coincides with a high variability of texture [3].

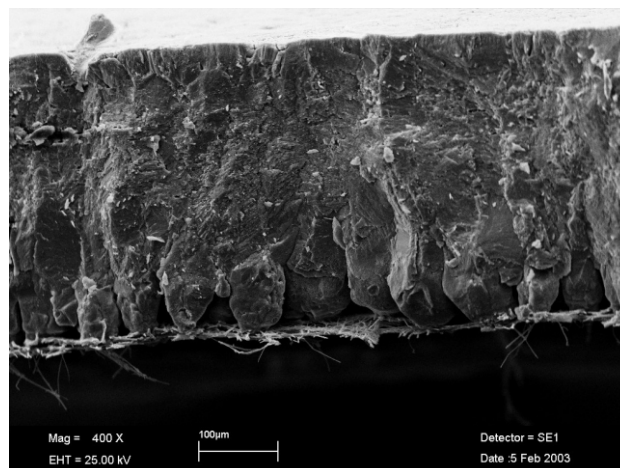


Figure 2. SEM picture of egg-shell. Outer side is on the bottom.



As a general conclusion and amazing fact, we can say that any differences of XRD parameters (for inorganic – calcite part) between the eggs of very different origin are not significant. So that their microstructure and composition, as they can be seen by XRD, are the same. All the shells investigated exhibited strong texture from outside and no texture from inside (Fig. 1). This agrees with the SEM pictures (Fig. 2) and known fact that from smaller more or less isotropical grains larger columnar grains are developed to the outer side. This work was an attempt for non-traditional application of powder diffraction with the aim to show that the method may be helpful also for biologists. Not only because of the phase analysis but also for the study of nanostructure of inorganic crystalline phases in biological objects. This is closely related to the overall microstructure strongly influenced by proteins taking part in its creation. The egg-shell matrix proteins influences the process of crystal growth by controlling size, shape and

orientation of calcite crystals. The formation of avian eggs belongs to most rapid mineralization processes known.

1. R. B. Von Dreele, "Combined Rietveld and Stereochemical Restraint Refinement of a Protein Crystal Structure," *Journal of Applied Crystallography* **32**, 1084-1089 (1999).
2. <http://lansce.lanl.gov/research/vondreele.html>.
3. Y. Nys, J. Gautron, M. D. McKee, J. M. Garcia-Ruiz, M. T. Hincke, Biochemical and functional characterisation of egg shell matrix proteins in hens. *World's Poultry Science Journal* **57** (2001) 401-413.
4. R.M.G. Hamilton, The Microstructure of the Hen's Egg Shell - A short review, *Food Microstructure* **5** (1986), 99-110.
5. P. Hunton, Understanding the architecture of the egg shell, *World's Poultry Science Journal* **51** (1995) 141-147. *Materials Structure*, vol. 10, number 1 (2003) 39.

